

## Algorithms of building lineaments in the program GIS-ENDDB

I.I. Kalinnikov, A.V. Mikheeva

**Abstract.** In this paper, we show one of recent GIS-ENDDB algorithms: the algorithm of building seismicity lineaments in terms of Great circles of the Earth. We also show using some other GIS-ENDDB algorithms to identify and to confirm the possibility of existence of global tectonic structures of the lineament type in different geodynamic regions. The formalized lineament construction based on fundamental physical laws allows us to reconstruct the long-term geological processes within a single mechanism of the structure formation. Examples of application of this GIS-ENDDB algorithm show the importance of developing the methods of the lineament construction to solve fundamental geodynamic problems.

**Keywords:** catalog of the earthquakes, tectonogenic structure elements, geophysical anomalies, seismicity lineament.

The geographic information system GIS-ENDDB [1] that was developed for geophysicists enables the researcher to operate to his choice with multiple components of geophysical processes. These processes are multi-dimensional and nonlinearly related; they are of different scales and dynamically developing. The researcher cannot take into account all the factors affecting the dynamics of real geophysical manifestations, so in the results interpretation he is always in terms of an ambiguous and undefined choice. Such a state of affairs is an unavoidable consequence of the dynamics of multi-dimensional nonlinear systems, which exhibit the capacity for self-organization and bifurcation. The more powerful is the GIS, the better the researcher's needs is realized to gradually, step by step, choose the most reliable of many possible variants.

In this paper, an attempt is made to illuminate this kind of problems in one of recent GIS-ENDDB algorithms: the algorithm of building seismicity lineaments in terms of Great circles of the Earth. We also show using some other GIS-ENDDB algorithms to identify and to confirm the possibility of existence of global tectonic structures of the lineament type in different geodynamic regions. Among the latest updates into the GIS-ENDDB subsystems of information and mathematical software used in this study, there are algorithms of constructing contours of maximum earthquake magnitudes and functions of visualization of geophysical fields.

## 1. Methods of structural-lineament construction

The formalized algorithm of building lineaments is based on underlying physical principles of the environment destruction: the causal conditionality expressed in a chronological sequence of spatially related events, the requirement of a potential energy minimum of the discontinuity surface, and the statistical reliability provided by events of a lineament. Despite the fact that the geophysical environment is not isotropic and has a block-layered structure and the stress field is non-uniform, the final implementation of the actions of physical laws at the global (inter-regional) scale should tend toward the lineaments, i.e. to geometrical shapes, providing a surface energy minimum. These shapes are “planes”, “cylinders”, and “spheroids”, as well as “lines” and “dendrite-like” cracks [2]. In this case, the lineaments reflect the results of geological processes, only partially enclosed by the instrumental seismic data (available only for the last century), and in our opinion allow us to reconstruct the long-term geological processes within a single mechanism of structures formation not yet accepted in geology [3].

By now, within the GIS-ENDDB, two algorithms for detecting linear structures corresponding to the active (in a given time period) fault system have been developed.

As for the first algorithm using a set of points distributed in space, linear images are detected based on the assignment of a minimum number of points in the chain  $n_{\min}$ , a maximum step  $L$  (in km), and a maximum deflection of the angle  $Az$  (in degrees) for the chronological searching for the next point (the event epicenter) [4]. This algorithm is conventionally called the method of pattern recognition (PR). Earlier, this algorithm was described [5] on an example of its use in identifying a system of transform lineaments of the major earthquakes in Central Asia (in the temporal interval of 2,250 years). This example shows that a lineament is not only a rupture in the monolith, but an elongated bandpass structure with anomalous geophysical properties extending along the Great circle of the Earth within which seismicity is migrating (Figure 1).

Thus, the second method of lineament constructions was offered. It also involves the validity of the fundamental physics laws in the global geodynamic processes (the above-mentioned principle of the least action, which requires the destruction of a uniform environment on planes, cylindrical and spherical surfaces in cases of a linear and a point loads), in particular, on segments of the Great circle (GC) if a discontinuity overcomes the Moho layer.

Let us list the main provisions of the new algorithm (conditionally called GC) having only two defined parameters: the number of points in the chain  $n_{\min}$  and a maximum distance between the reference events  $L$  (in km). The first parameter provides statistical representation of building and the second

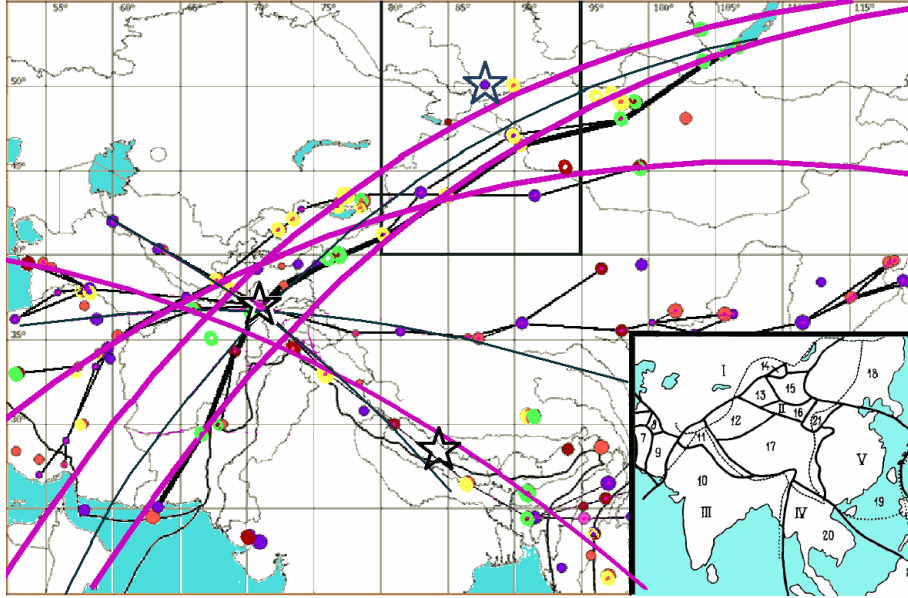


**Figure 1.** The PR-lineaments system of the Arabian Plate—the Baikal Rift Zone—the Himalayas [4] and the corresponding GC-lineaments: Significant Catalog; –250–2008 years, a bright broken line shows the “African–Baikal” PR-lineament [5], the thick arc lines are GC-lineaments constructed with the parameters  $(L, n_{\min}) = (3,400 \text{ km}, 19)$ ,  $M \geq 7.2$ , and  $15 \leq H \leq 80 \text{ km}$ ; the thin arc lines are the “axial” GC-lineaments of a more local level:  $(L, n_{\min}) = (1,000 \text{ km}, 14)$ ,  $M \geq 6.5$ , and  $H \leq 100 \text{ km}$ . In the inserted pictures, the scheme of borders of plates and microplates (I–V—large plates, 1–20—small plates, solid and dotted lines according to different authors) [6]. The asterisks mark the epicenters of Chui earthquake (27.09.2003,  $M_s = 7.5$ ), Pamir Hindu Kush seismofocal zone, and the Nepal event (25–28.04.2015)

geometrical one takes into account the effect of sphericity of the Earth’s crust at distances of  $L$ , which, at least, twice should exceed the size of the focal zone of the strongest earthquakes and must be many times greater than the thickness of the Earth’s crust:

1. Suppose that  $N_{\max}$  is the total number of selected events (for example, only the crust ones) from the ancient times with  $M_{\max} - 2 \leq M \leq M_{\max}$ , and a predetermined depth as well as with a random spatial distribution and a temporal distribution variance of  $\sqrt{N_{\max}}$ .
2. Calculate  $R(1, i)$ , i.e. the distance between the chronologically first and all the subsequent events.
3. Repeat Step 2 for all the subsequent events until the number of columns is  $N = 3\sqrt{N_{\max}}$ . As we expect, this sample ensures the presence of, at least, one strong event with its fault.

4. Select all the events (from each of  $N$  columns), where every two chronologically successive ones are located not closer than  $L/2$ .
5. Between each two chronologically close events satisfying the condition posed on the distance  $L/2 \leq R(j, i) \leq L$  we assume the presence of a stress field, which may generate an elongated tectonic fault with a minimum surface energy, i.e., throughout the Great circle. Therefore, through each pair of such events and the Earth's center we build a plane dissecting the lithosphere by the Great circle.
6. Compute a distance to all the events in the catalog for all the planes constructed, selecting the GC planes with a sufficient number ( $n \geq n_{\min}$ ) of closely located events (with a fixed distance from the plane:  $\Delta D \leq L/20$ ).

The algorithm implies the expert skill in setting the events selection and the control parameters  $\Delta D$  and  $L$  taking into account many complicated factors: different reliability of data on modern and ancient earthquakes; uncertainty of the criteria for throwing away the clearly false candidates for lineaments. The advantage of the algorithm is its speed relative to the

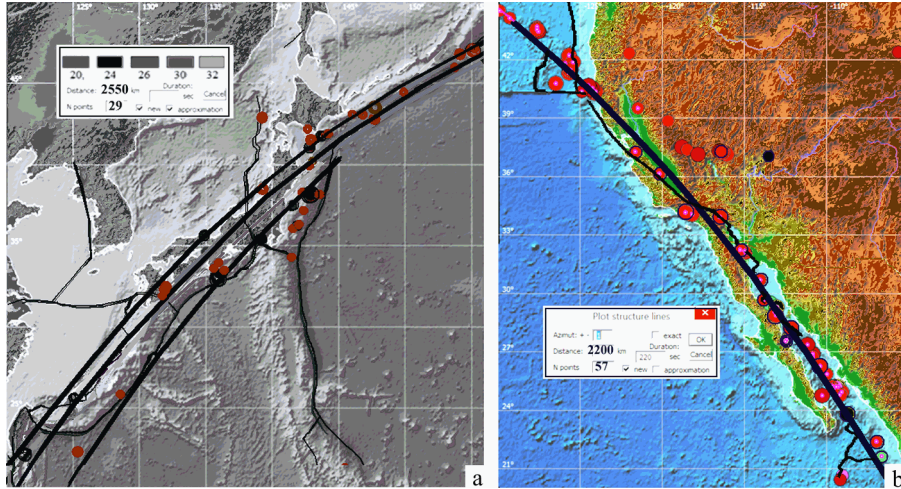


**Figure 2.** The GC-lineaments of different seismic-prone regions: a) sub-parallel “Taiwan Kuril” lineaments constructed according to the Japanese catalog JMA with the parameters  $(L, n_{\min}) = (2,550 \text{ km}, 29)$ ,  $h = 87.9$ ,  $7 \leq M \leq 9$ , and  $15 \leq H \leq 40 \text{ km}$ , 1923–2013, whose influence zone includes the Great East Japan Earthquake ( $M = 9$ ) and the recent strongest events of the region ( $M = 7$ ,  $32.78^\circ \text{ N}$ ,  $130.73^\circ \text{ E}$ ; 2016.04.14, 16:25), and, also, the lineament  $(L, n_{\min}) = (1,500 \text{ km}, 24)$ ,  $h = 62.5$ , coinciding with the north-eastern boundary of the Philippine Plate; b) the “Californian” lineament according to the English catalog ISC:  $(L, n_{\min}) = (2,200 \text{ km}, 57)$ , coinciding with the interplate border and most provided with the events

previous version (PR), which enables in the manual sorting mode to carry out the optimization search for significant Great circles (GC), for example, by the criterion of a minimum of the relationship  $h = L/n_{\min}$  or a definition of the width of a fault zone  $\Delta D_{\max}$ . In both these cases, the choice should correspond to the real geophysical environment. Figure 2 presents the GC-lineaments corresponding to local minima of  $h$ . They are associated with the known boundaries of tectonic plates, i.e., meet the criterion of fault deepness.

Moreover, the expert study should be carried out together with the interpretation of existing geophysical fields allowing specify the selection criterion of the candidate for reliable lineaments. For example, by varying  $h$ , we can build different versions of the “Taiwan-Kuril” GC-lineaments covering the latest earthquakes or corresponding to the known interplate (transform) faults (see Figure 2a).

Currently, the GC-algorithm is being tested on real seismicity material in Central Asia, the Pacific subduction zone and other seismic-prone regions (Figure 3). According to Figures 1 and 3b, the obtained GC-arcs confirm the correctness of the global lineaments system (broken lines) selected by the first pattern recognition algorithm (PR), in particular, the most extended “African–Baikal” lineament (see Figure 1) and its “Chui” fragment (Figure 3b).

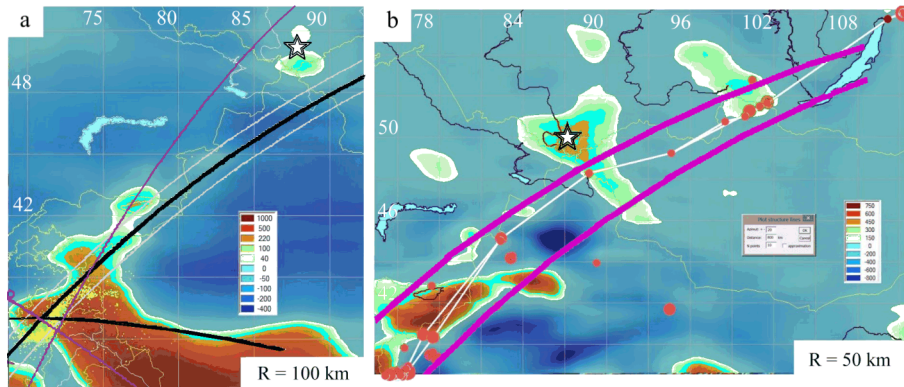


**Figure 3.** The association of seismic lineaments and the edges of gravity anomalies heights (the regional component of the gravitational field with a specified averaging radius): a) the “axial” GC-lineaments (see, also, Figure 1) in the Central Asian region (with its interval  $\Delta D$ ) and the “Eurasian-Indian” lineament:  $SIGN, 6.6 \leq M \leq 8.8, 16 \leq H \leq 70 \text{ km}, -2250-2015 \text{ y}, (L, n_{\min}) = (1000 \text{ km}, 11)$ , in the north covering the Chui earthquake, and in the south – the Eurasian-Indian interplate boundary; b) the “Chui” cluster identified by PR-algorithm:  $(Az, L, n_{\min}) = (20^\circ, 800 \text{ km}, 10), M \geq 3$ , in September, 2003, with related GC-lineaments (see, also, Figure 1). The asterisks mark the epicenter of the Chui earthquake

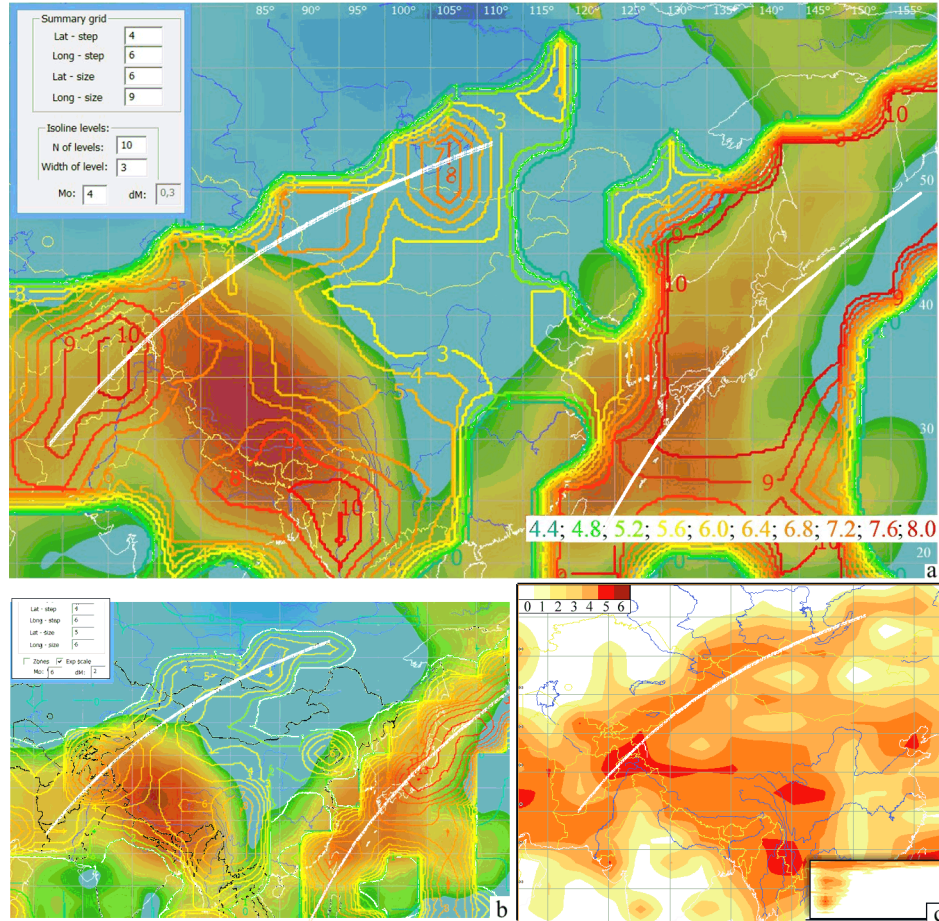


**Figure 4.** Isolines of the  $M_{\max}$ , of the number of events, and of the total energy according to COMPLEX catalog,  $4 \leq M \leq 8$  on the background of the map of a regional component of the heat flow obtained by the same averaging: a)  $M_{\max}$ -contours for events of  $H \geq 34$  km, the averaging cell is  $6 \times 9^\circ$ ,  $4 \times 6^\circ$  step (contour lines 1–10 correspond to the magnitude of  $M = 4.0\text{--}4.4, \dots, 7.6\text{--}8.0$ , respectively); b) isolines of the number of events per unit area (the averaging cell is  $5 \times 6^\circ$ , isolines 0–11 correspond to the upper value of  $N = 6, 48, 69, 100, 147, 218, 324, 483, 721, 1,078, 1,615$ , and  $2,419$  according to the power scale with the steps  $\Delta N = (N_{\max} - N_{\min}) \cdot 1.5n + 2$ ,  $n = 1, 2, \dots$ ); c) contour lines of the total energy released per unit area on the map (averaging cell is  $3 \times 5^\circ$ , isolines 1–6 correspond to the upper value of  $E = 45 \cdot 10^4, 47 \cdot 10^5, 49 \cdot 10^6, 52 \cdot 10^7, 54 \cdot 10^8, 57 \cdot 10^9$  Joules/year/km<sup>2</sup>) and in the cross-section (by the profile along the lineament,  $H_{\max} = 300$  km). GC-lineaments are also shown: “Taiwan Kuril” (a–b) (see, also, Figure 2a) and “African-Baikal” (c) (see, also, Figure 1)

Let us note that mapping the lineaments on the background of GIS-ENDDDB maps in terms of digital gravimetric models of RSD (Remote Sensing Data) allows us to discover its association with inhomogeneities of a gravitational field, in particular, with the borders of a maximum gradient of these anomalies. It is especially evident on the background of the regional component (see Figure 3) presumably related to lateral inhomogeneities in the upper mantle [7].

In addition, as Figure 4 shows, the “African-Baikal” GC-lineament is confirmed by the statistical analysis, for example, by  $M_{\max}$ -contour configuration (maximum earthquake magnitudes), where the lineament structure even more extended to the north-east (up to the Viluy-Lena watershed). From this corner point, the linear structure extends over the Baikal rift zone (BRZ) to the south-west with value 8 of a maximum intensity (i.e.,  $M_{\max} \leq 7.2$ ) in the BRZ, and 10 (i.e.,  $M_{\max} \leq 8$ ) in the Pamir Hindu Kush area (PHK) (see Figure 4a). The “African-Baikal” lineament is also detected by contours of the number of all the earthquakes (including the crust events) (see Figure 4b) as well as by contours of the total energy released per unit area (see Figure 4c).

At the same time, the averaging parameters presented in Figure 4a show a good coherence between contour configuration of  $M_{\max}$  (constructed without taking into account the earthquakes of more “fragile” top layer of the Earth’s crust) and the regional component of the heat flow field. Such a coherence may indicate to the relationship of averaged characteristics of the depth seismicity with the thermal field and can be indicative of controlling the depth seismicity from thermal processes in the upper mantle.

The deep mantle processes can control the activation identified in the lineament structures (also, being complicated by the interplate collision processes), which can have various activities in different time epochs. In particular, one of the branches of the “African-Baikal” lineament system stretching to the south-east of the PHK zone (“Nepali” lineament) passes exactly through the epicenter of the recent Nepal multi-earthquake (25–28.04.2015,  $M_w = 7.8$ ) (see Figure 1). This branch stably manifested in lineament constructions in the whole 2000-year observation period (see Figure 1) and in the last 100- and 10-year periods (Figure 5). In the last 10 years, this branch manifested itself as the most active lineament on the background of a relative calm of other branches (see Figure 5b).

Thus, the lineament construction algorithm (as combined with the methods of statistical analysis of the seismic regime characteristics and with the geographic information methods of the geological and geophysical data visualization) helps us to solve not only the fundamental problems of geodynamics, but also the prognostic application tasks. In particular, the algorithm in question can help in finding new patterns of seismic activity preparation, identifying long-term precursors (as in the example of the Nepal earthquake),

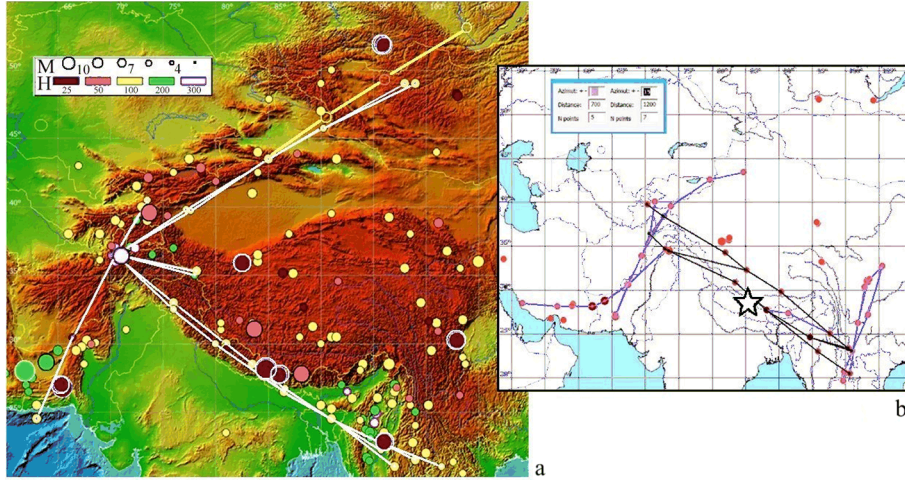


**Figure 5.** The PR-lineaments for the major seismic activity in Central Asia of the last 100- and 10-year periods: a) according to the ISC catalog for 1905–2011:  $M \geq 6.5$ ,  $20 \leq H \leq 300$ ,  $(Az, L, n_{\min}) = (5^\circ, 800 \text{ km}, 25)$ , since 2005 the size of events increased by the factor of 2; b) according to the NEIC catalog for 2005–2015:  $M \geq 6$ , gray:  $(Az, L, n_{\min}) = (20^\circ, 700 \text{ km}, 5)$ , black:  $(Az, L, n_{\min}) = (15^\circ, 1,200 \text{ km}, 7)$ . An asterisk indicates to the Nepal events (25–28.04.2015)

and, if there are high quality seismic catalogs, the short-term ones of the future disruptive events (as in the example of the Chui cluster, which was a short-term precursor of the major Chui earthquake [1]).

## 2. Conclusion

The formalized lineament construction based on fundamental physical laws allows us to reconstruct the long-term geological processes, for example, within a single mechanism of the structure formation, which is not so far accepted in geology. Examples of application of the GIS-ENDDB tools show the importance of developing the methods of the lineament construction to solve fundamental geodynamic problems. They assume a more significant role of the fundamental laws of the determined action in geodynamics and, on this basis, to refine the boundaries of plates, to indicate the probable transform boundaries created or activated by converging plates, to assess their effect on the geodynamic regime of the surrounding areas, and to clarify the width of transform plate zones defined by branching lineaments.

On the other hand, the detailed study of the lineaments dynamics in the preparation zone of potential earthquakes at minor intervals and a low energy level can give a lot of prognostic information to seismologists. Undoubtedly, using GIS-ENDDB the system will benefit to studying various

natural disasters of any scale in terms of their manifestations in modern geomorphology and geotectonics, and, perhaps, in terms of their prediction.

## References

- [1] Mikheeva A.V. *Geostructural Elements Detected by Mathematical Algorithms and Numerical Models of the Geoinformation-Computer System GIS-ENDDB*.—Novosibirsk: Omega Print, 2016 (In Russian).
- [2] Oparin V.N. et al. *The Zonal Disintegration of Rocks and Stability of Underground Workings*.—Novosibirsk: Publishing House of the SB RAS, 2008 (In Russian).
- [3] Ustyantsev V.N. *On a Single Mechanism of Structure Formation of the Earth System*.—LAMBERT, 2013 (In Russian).
- [4] Dyadkov P.G., Mikheeva A.V. *Methods for detection of spatial clustering of earthquakes in seismogeodynamic study areas of Central Asia // Mathematical methods of pattern recognition: The 15th All-Russian Conference (Petrozavodsk, September 11–17, 2011): Proc. rep.*—Moscow: MAKS Press, 2011.—P. 560–563 (In Russian).
- [5] Kalinnikov I.I., Mikheeva A.V. *The GIS-EEDB computing system, lineaments and a problem of earthquake prediction // Bull. Novosibirsk Comp. Center. Ser. Math. Model. in Geoph.*—Novosibirsk, 2015.—Iss. 17.—P. 17–34.
- [6] Nikolaev N.I. *The Newest Tectonics and Geodynamics of the Lithosphere*.—M.: Nedra, 1988 (In Russian).
- [7] Mikheeva A.V., Kalinnikov I.I. *Geo-structural elements detected by digital models and formal algorithms of the GIS ENDDB // Proc. 10th International Seismological School “Modern methods of processing and interpretation of seismic data” (Novhany, Azerbaijan, 14–18 September 2015)*.—2015.—No. 17.—P. 221–225 (In Russian).

